sustainability

MDPI

Review

The Potential of rGO@TiO_2 Photocatalyst for the Degradation of Organic Pollutants in Water

Martina Kocijan [1,*], Lidija Ćurković [1,*], Gil Gonçalves [2,3] and Matejka Podlogar [4]

[1] Faculty of Mechanical Engineering and Naval Architecture, University of Zagreb, Ivana Lučića 5, 10000 Zagreb, Croatia
[2] Centre for Mechanical Technology and Automation, Department of Mechanical Engineering, University of Aveiro, 3810-193 Aveiro, Portugal
[3] Intelligent Systems Associate Laboratory (LASI), 3810-193 Aveiro, Portugal
[4] Department for Nanostructured Materials, Jožef Stefan Institute, Jamova Cesta 39, SI-1000 Ljubljana, Slovenia
* Correspondence: martina.kocijan@fsb.hr (M.K.); lidija.curkovic@fsb.hr (L.Ć.)

Abstract: The availability of clean water is essential for humans wellbeing and the diverse biotic population in the environment. Menkind imposes a significant pressure on food supplies, natural resources, and other commodities. Large-scale anthropogenic activities, such as agriculture and industry, which are practiced to ensure population growth and survival, have caused several harmful environmental effects, including the discharge of pollutants into the aquatic environment. Among them organic micropollutants (OMPs) are considered a significant threat to aquatic ecosystems. The efficient removal of this persistent pollutants from wastewater is nowadays commonly considered in water treatment technologies. Utilizing photocatalysis by harvesting solar energy as an inexhaustible source, represents a facile and easy to upscale solution, for removing persistent pollutants and other emerging contaminants. In the recent decade, graphene-based titanium dioxide catalyst (rGO@TiO_2) has received a lot of attention as an effective material for the degradation in the enviroment. This review summarizes the recent progress in preparing rGO@TiO_2 nanocomposites and their utilization for purification purposes. Its main advantage over many other photocatalysts is its easy preparation, low toxicity, and reasonable photo-activity in a specific solar light spectrum.

Keywords: graphene; semiconductor; photocatalytic degradation; nanocomposite; water treatment; organic pollutants

check for updates

Citation: Kocijan, M.; Ćurković, L.; Gonçalves, G.; Podlogar, M. The Potential of rGO@TiO_2 Photocatalyst for the Degradation of Organic Pollutants in Water. *Sustainability* **2022**, *14*, 12703. https://doi.org/10.3390/su141912703

Academic Editors: Hugo Cruz, Gonzalo Guirado, Karolina Zalewska Patricio, Luis Cobra Branco and Dino Musmarra

Received: 10 August 2022
Accepted: 29 September 2022
Published: 6 October 2022

Publisher's Note: MDPI stays neutral with regard to jurisdictional claims in published maps and institutional affiliations.

Copyright: © 2022 by the authors. Licensee MDPI, Basel, Switzerland. This article is an open access article distributed under the terms and conditions of the Creative Commons Attribution (CC BY) license (https://creativecommons.org/licenses/by/4.0/).

1. Introduction

Today, clean water sources represent the highest priority for the sustainability of the entire ecosystem [1–3]. Environmental issues that are related to water pollution raise a serious concern over the last couple of decades due to the expanding industrial and agriculture activities [4–7]. Toxic organic pollutants amassed in our proximity have a negative effect on the biotic habitat and even human health. It is still extremely difficult to envision the elimination of these persistent pollutants which were found virtually in all water bodies [8–10]. Among them, persistent organic micropollutants (OMPs) such as organic dyes (i.e., methylene blue (MB), methylene orange, congo red), pesticides, pharmaceuticals, and their metabolites were proven extremely toxic [11]. The waste consisting of OMPs is also deemed problematic due to its difficulty for removal, low biodegradability, and long degradation lifetime in the ecosystem [12].

Conventional wastewater methods such as adsorption, biological treatment, filtration, chemical treatment, flocculation, etc., are not efficient enough to degrade especialy aromatic and heterocyclic groups in their moleculear structure [13,14]. The remediation should consider degradation and mineralization of this contaminants to its highest stable oxidation state such as: water, carbon dioxide, and the oxidized inorganic anions or into less toxic and also easily degradable species, that can be remediated through naturally pathways [15].

Therefore, extensive efforts have been directed globally toward the development of suitable, efficient, and eco-friendly processes for the removal of persistent pollutants. Nevertheless, strategies are being continuously developed for their remediation [16,17]. The task at hand is to choose an efficient and environmentally benign method, which would clean wastewater of its toxic ingredients. Recent research is focused on the advanced oxidation process (AOP) utilizing semiconductor nanoparticles with appropriate physical and chemical properties which would enable photocatalysis [18–20].

1.1. Challenges of TiO_2 Semiconductor Photocatalysts

Titanium dioxide (TiO_2) represents a well-studied photocatalyst that has been widely considered in research activities and is also commercialized. Because of its appealing physical and chemical properties, it was found useful in a wide spectrum of applications. Its thermal and chemical stability makes it resistant and unproblematic in the environment, it has good mechanical properties, and with respect to photocatalytic processes, it exhibits great activity under ultraviolet (UV) light irradiation (<387 nm) [21,22]. However, utilization of TiO_2 in a wider sunlight spectrum, which has its maximum in the visible range, requires a decrease of its bandgap energy, whilst inhibiting the recombination of photogenerated electron (e^-)—hole (h^+) pairs. Among the many approaches composite based on graphene and graphene-like materials (GO, rGO) addresses major limitations of TiO_2 [23–26]. Coupling TiO_2 with narrow bandgap materials with the visible light response is important to obtain an effective nanocomposite for photocatalytic applications. The synergistic effect between materials constituting nanocomposite improves visible light response, charge separation, and thus photocatalytic activity. On top of all both species were found way less harmful to the environment.

The mechanism of semiconductor photocatalysis can be divided into three steps (Figure 1). Firstly, using irradiation with the required energy (wavelength), electron (e^-)—hole (h^+) pairs are produced within the TiO_2 semiconductor particles. Furthermore, photogenerated charges must diffuse to the surface of the TiO_2 hence the low recombination rate. Lastly, generated electrons (e^-) and holes (h^+) must have the right reductive and oxidative potential to initiate chemical reactions driven through the surface of the catalyst. These reactions subsequently transform OMPs into low or non-toxic compounds [27,28].

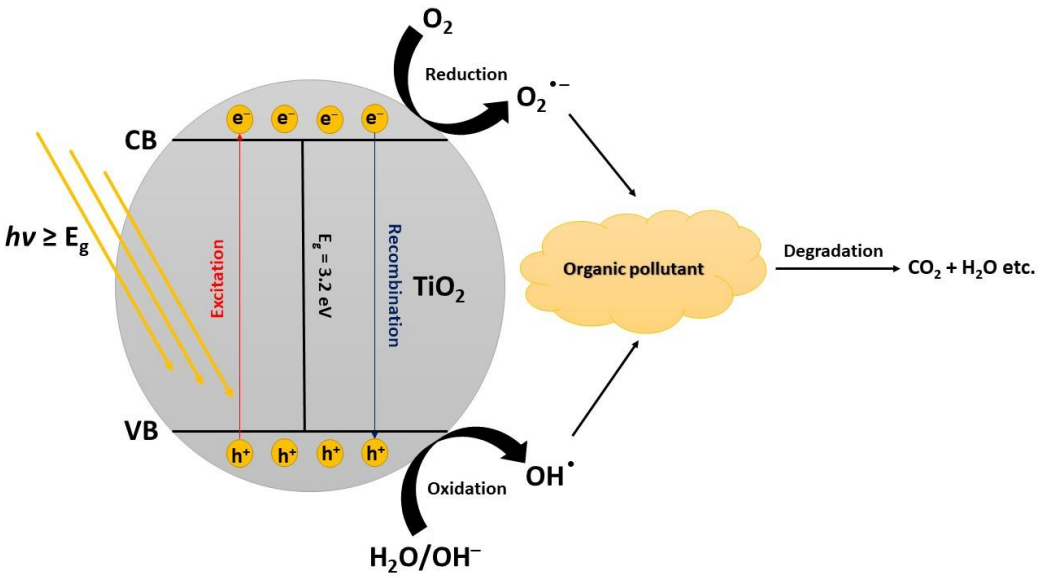


Figure 1. Photocatalytic reaction mechanism on TiO_2 semiconductor material.

While papers related to rGO-based TiO_2 photocatalyst are continuously being published, a review in front of you is aimed at summarizing recent work on nanocomposites. More precisely, the main objective is to highlight few synthesis methods of graphene-based

TiO_2 nanocomposites formation and their operation characteristics for efficient photocatalytic water purification treatment. This work also summarizes few research conducted on diverse water bodies, which represents an important step towards practical application.

1.2. Why Coupling TiO_2 with Graphene?

Graphene is a single layer of sp^2-bonded carbon atoms firmly packed into a two-dimensional honeycomb structure. It is an allotrope of carbon, with extraordinary properties, such as large theoretical specific surface area (2630 $m^2\ g^{-1}$), optical transparency, high Young's modulus (~1 TPa), high carrier mobility at room temperature (~10,000 $cm^2\ V^{-1}\ s^{-1}$), and excellent thermal conductivity (3000–5000 $W\ m^{-1}\ K^{-1}$) [26,29,30]. Graphene has been widely used to improve the catalytic efficiency of photocatalysts. The photogenerated charge carriers are separated and the recombination rate of electrons/holes is reduced, thus the lifespan of charge carriers is extended. As a result, more reductive electrons and oxidative holes are accessible for the reaction, and the photocatalytic activity is enhanced [29,31–33].

Graphene Oxide (GO) is a valuable derivative of graphene. It consists of also oxygen and hydrogen and their functional groups which are attached to the hexagonal carbon skeleton thus disrupting the perfect sp^2 hybridization. The process of partial sp^2 bond recovery produces another important hybrid of carbon named reduced graphene oxide (rGO). Ideally, GO consists of a single carbon layer structure with oxygen containing functional groups positioned in or out of the hexagonal skeleton plane. However, most often GO is composed of multilayers. In contrast to perfect graphite consisting of single graphene layers connected through van der walls bonds, carbon layers are intercalated with oxygen functional groups and their bonds. GO is also considered two-dimensional carbon material; however, its properties are far from that of graphene. It does not absorb visible light, has very low electric and thermal conductivity compared to graphene, and demonstrates significantly higher chemical reactivity due to the presence of oxygen species [33–35]. Graphene can be oxidized to consist of several different oxygen functional groups such as epoxy, carbonyl, carboxyl, and hydroxyl, which play a relevant role in catalytic applications. The physicochemical properties of GO can be significantly changed according to the oxidation process applied [36]. By this, we can control the concentration of defects in the carbon structure Ref. [37]. By exploring several chemical [38] or physical treatments, ref. [39] GO can be converted in rGO which is in terms of physic-chemical properties an intermediate material of GO and graphene and deserve its own labeling. The molecular structures of graphene and its derivates (GO and rGO) are shown in Figure 2.

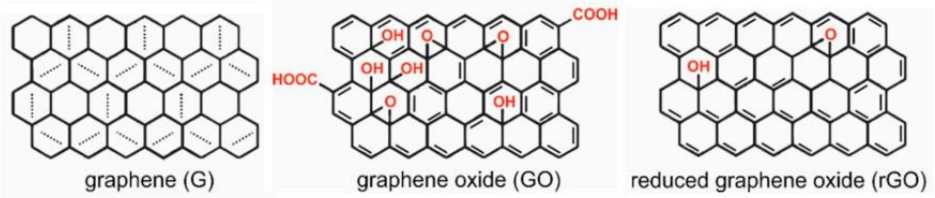


Figure 2. Graphical representation of the molecular structures of graphene material and its derivates [40].

GO and rGO have been usually synthesized using natural graphite flakes as a precursor material and in the following section, the most common approaches to synthesizing them will be discussed.

1.2.1. Synthesis of Graphene Oxide (GO)

Carbon has fascinated chemists already a very long time ago and in 1859 Benjamin Brody synthesized GO from graphite flakes using $KClO_3$ and HNO_3 [41], even though graphene was not discovered at that time yet. In 1898, Staudenmaier [42] has slightly modified Brody's method by using a concentrated H_2SO_4 in the presence of $KClO_3$ and HNO_3. In 1958, Hummers [43] has improved the existing process of GO production by

using strong oxidizing agents such as $KMnO_4$ and $NaNO_3$ and the obtained product was a higher yield and better purity in comparison to the product from previous methods. The reported methods are very simple for synthesis, however, a major drawback is the formation of several toxic components (NO_2, N_2O_4, and ClO_2) during the process [44]. In 2010, Marcano et al. [45], prepared GO material by implementing several changes to Hummers' method, called modified Hummers' method and improved Hummers' method, using natural graphite flakes (~150 μm).

In the last decade, many researchers worldwide have given attention to GO used for many applications obtained via different approaches of the Hummers' method due to its higher yield in the production of GO [46–50]. All these reports implicate that excellent knowledge of the synthesis of GO material is of paramount importance for obtaining a material with desirable properties for targeted applications.

1.2.2. Reduction of GO to rGO

Through the reduction of GO to rGO, functional groups of oxygen (hydroxyl, carbonyl, carboxyl, and epoxy) can be removed. Since these methods can greatly transform the microstructure and properties of GO, several successful reductions have been performed by chemical [51,52], thermal [51,53], sonochemical [54], electrochemical [55], and photochemical [56] methods.

The most common transformation of GO into rGO is through thermal annealing. The oxygen-containing functional groups decompose during high temperatures into gases. These gases can produce high pressure between the stacked layers. According to the reported research [57], pressures of 40 MPa and 130 MPa are produced at 300 °C and at 1000 °C, respectively.

1.2.3. Preparation of rGO-Based TiO_2 Photocatalyst

rGO-based TiO_2 material is commonly used in light-driven photocatalysis of dyes in an aqueous medium. Because of exceptional properties, rGO-based oxide semiconductors promote electron separation, which results in boosting photo-driven reactions such as the degradation of carcinogenic dyes (e.g., methylene blue) and solar-fuel (hydrogen) production. Preparation of rGO-based TiO_2 photocatalysts increases the specific surface area of the nanocomposite, consequently increasing the photocatalytic activity, which is why rGO-based semiconductor photocatalysts have been found to be promising in several applications. In the last decade, many studies have reported on improved photocatalytic activity on OMPs degradation. In these studies, rGO has been coupled with TiO_2, the well-recognized semiconductor material, to enhance their performance in the photodegradation processes of OMPs from water bodies [58–60].

Nowadays, the rGO-based TiO_2 nanoparticles are synthesized by physical as well as chemical methods such as sol-gel, hydrothermal and solvothermal techniques and by calcination treatment, hydrolysis, etc. The sol-gel method is a simple and cheap synthesis process that provides homogeneity to the prepared nanocomposite and is performed at very low temperatures. Preetha et al. [61] has reported the synthesis of rGO@TiO_2 nanocomposite by the sol-gel method using titanium (IV) isopropoxide (TTIP) as a precursor in an ethanol medium followed by calcination treatment. Different weight percentages of GO were dispersed before the sol-gel reaction. The hydrothermal/solvothermal technique is one of the simplest synthesis techniques widely adopted for the preparation of nanocomposite photocatalysts. The morphology and physicochemical properties are significantly affected by the hydrothermal conditions such as duration of synthesis, temperature, cooling conditions, used precursors, etc. [26]. The high pressure used in the hydrothermal/solvothermal technique leads to good interactions between used precursors and can be performed at even lower temperatures. The synthesized nanocomposite exhibits synergy in properties of individual components which are attractive in photocatalytic degradation. During the hydrothermal/solvothermal technique, GO is mixed with a precursor in solution, where the latter transforms into small crystals on the surface of graphene [62]. Several

authors reported how enhanced degradation of organic pollutants can be achieved using such composite prepared by this simple and cost-effective hydrothermal technique followed by calcination treatment (Table 1). Another case of enhanced photocatalytic degradation, of methylene blue and rhodamine B in an aqueous medium [63], was observed using self-assembled rGO@TiO_2 nanocomposite synthesized by a one-pot hydrothermal technique using TTIP and GO at 180 °C for 6 h followed by calcination treatment at 300 °C for 2 h. Wanag et al. [25] reported a two-step solvothermal technique followed by calcination treatment for the preparation of rGO@TiO_2 photocatalyst nanocomposites with improved photocatalytic degradation. Sohail et al. [64] reported a simple hydrolysis method for preparing the same composite using titanium butoxide as a precursor in ethanol which was added to the GO suspension after which the obtained precipitates were calcined at 500 °C for 2 h.

Table 1. Photocatalytic degradation of organic pollutants by rGO@TiO_2 nanocomposite.

Synthesis Method	Catalyst Dosage	Light Source	Pollutant and Initial Concentration	Irradiation Time	Kinetic /10^{-3}	Removal Efficiency	Reference
Solvothermal	0.8 g/L	UV light	Methylene blue, 10 mg/L	90 min	-	100.0%	[25]
Sol-gel method	0.5 g/L	Natural sunlight	Alizarin Yellow GG, 10 mg/L	150 min	-	100.0%	[61]
Hydrothermal	0.5 g/L	Simulated solar light	Rhodamine B, 10 mg/L	120 min	53.1 min^{-1}	99.8%	[63]
Hydrothermal	0.5 g/L	Simulated solar light	Methylene blue, 10 mg/L	120 min	32.84 min^{-1}	98.1%	[63]
Sonochemical	2.0 g/L	Natural sunlight	Methylene blue, 20 mg/L	30 min	18.8 min^{-1}	91.3%	[65]
Solvothermal	0.1 g/L	Natural sunlight	Methylene blue, 15 mg/L	60 min	21.2 min^{-1}	85.0%	[66]
Solvothermal	0.1 g/L	UV lamp	Methylene blue, 15 mg/L	60 min	89.1 min^{-1}	100.0%	[66]
Hydrothermal	0.075 g/L	Natural sunlight	Diclofenac, 25 mg/L	60 min	50.4 min^{-1}	~100.0%	[67]
Hydrothermal	0.1 g/L	UV light	Methylene blue, 12 mg/L	180 min	13.1 min^{-1}	~90.0%	[68]
Hydrothermal	0.0004 g/L	UV light	Methyl orange, 30 mg/L	30 min	122.0 min^{-1}	95.0%	[69]
Hydrothermal	0.5 g/L	Visible light	Methyl orange, 10 mg/L	240 min	126.0 min^{-1}	87.4%	[70]
Hydrothermal	0.1 g/L	UV-A lamp	Clofibric acid, 20 mg/L	360 min	11.2 min^{-1}	100.0%	[71]
Hydrothermal	0.18 g/L	Simulated sunlight	Formalin, 40 mg/L	90 min	17.9 min^{-1}	93.8%	[72]
Freeze-drying	0.4 g/L	Simulated solar lamp	Rhodamine B, 10 mg/L	240 min	-	84.6%	[73]
Ultrasonication	0.75 g/L	UV light source	Methylene blue, 30 mg/L	120 min	-	99.3%	[74]
Solvothermal	0.1 g/L	Visible light	Methyl orange, 10 mg/L	180 min	-	94.1%	[75]
Hydrothermal	0.25 g/L	Simulated sunlight	4-nitrophenol, 45 mg/L	360 min	11.8 min^{-1}	95.0%	[76]
Solvothermal	1.0 g/L	UV light	Rhodamine B, 0.125 mM	300 min	6.3 min^{-1}	94.8%	[77]
Hydrothermal	0.5 g/L	UV-A lamp	Methylene blue, 6.4 mg/L	60 min	23.0 min^{-1}	86.0%	[78]
Hydrothermal	0.5 g/L	Natural sunlight	Methylene blue, 6.4 mg/L	60 min	20.0 min^{-1}	81.0%	[78]

Table 1. *Cont.*

Synthesis Method	Catalyst Dosage	Light Source	Pollutant and Initial Concentration	Irradiation Time	Kinetic /10^{-3}	Removal Efficiency	Reference
Sol-anaerobic calcination	0.4 g/L	UV light	Phenol, 10 mg/L	180 min	-	97.9%	[79]
Hydrothermal	1.2 g/L	Visible light	Humic acid, 30 mg/L	180 min	-	88.0%	[80]
Hydrothermal	0.5 g/L	Visible light	Methylene blue, 0.01 mM	130 min	37.4 min^{-1}	~99.0%	[81]
Hydrothermal	0.7 g/L	UV light	Ethylparaben, 0.3 mM	40 min	96.0 min^{-1}	98.6%	[82]
Hydrothermal	0.5 g/L	Natural sunlight	Bisphenol A, 0.01 mol/L	30 min	-	100.0%	[83]
Hydro-solvothermal	1.0 g/L	Solar light	2,4-Dichlorophenoxyacetic acid, 0.5 mM	180 min	9.6 min^{-1}	97.0%	[84]

2. Photodegradation of Organic Pollutants

In the recent decade, photocatalytic degradation of persistent OMPs such as dyes, pharmaceuticals, and pesticides into non-toxic and innoxious compounds (water and carbon dioxide) has become a hot research topic. Conventional wastewater treatment techniques present significate limitations in terms of complete degradation of the harmful OMPs as well as its high cost associated with the operational conditions. Indeed, with these techniques, it is very difficult to achieve the quality of treated water to a level required by the WHO organization [85].

Many studies using rGO@TiO_2 nanocomposite were made to improve photocatalytic efficiency. Liu [86] treated Methylene Orange (MO) using rGO@TiO_2 nanocomposite for 240 min exposing it to visible light ($\lambda > 400$ nm) irradiation and reported ~90% photodegradation of overall organic pollutant. Several authors report the photocatalytic degradation of methylene blue (MB) using rGO@TiO_2 nanocomposites, among them Deshmukh et al. [65] who got maximum degradation of MB equal to 91.3% within 30 min of sunlight irradiation. In another study by Mohammadi et al. [87], photocatalytic degradation of MB using rGO@TiO_2 composite was even better. 95% and 93% of the overall organic pollutant were removed within 30 min using irradiation from a 200 W Mercury short arc and Osram 500 W Xenon lamp with a cut-off UV filter at 400 nm, respectively. Furthermore, Garrafa-Gálvez et al. [66] studied the photocatalytic degradation of MB while using the same rGO@TiO_2 nanocomposites under natural sunlight and UV irradiation. They reported high effectiveness, 100% and 85% of MB of overall organic content under 60 min of UV and natural sunlight irradiation, respectively. Kusiak-Nejman et al. [88] investigated the same system but used UV-Vis light with higher UV intensity. The authors reported 91.48% of MB degradation after 60 min of UV-Vis light irradiation. Wu et al. [89] studied photocatalytic degradation of rhodamine B (RhB) using rGO@TiO_2 and reported ~95% removal within 90 min of UV irradiation (250 W high-pressure Hg lamp) at room temperature. The authors also studied nanocomposite reusability; the results obtained after five cycles indicate that the prepared nanocomposite is rather stable, with above 90% removal capabilities.

Reported studies also showed that the tailoring of rGO@TiO_2 nanocomposite morphology promotes improved photocatalytic efficiency for pharmaceutical and pesticide degradation. Balsamo et al. [84] reported 97% degradation of 2,4-dichlorophenoxyacetic acid (2,4-D) in 180 min using rGO@TiO_2 under solar light irradiation (Figure 3). The ion-spray ionization mass spectrometric (ISI-MS) analysis was utilized to show which by-products are formed. Figure 4. displays the ISI-MS spectra of prepared 2.4-D solution before (upper) and after performed photocatalytic test (bottom) using rGO@TiO_2 solar catalyst. After 3 h of continuous irradiation, 96% of removal was confirmed with the Total Organic Carbon (TOC) analysis. The ISI-MS spectra are done to investigate the formation

of by-products. After 3 h of continuous irradiation, 96% of removal was detected with the Total Organic Carbon (TOC) analysis. As confirmed by the ion-spray ionization mass spectrometry (ISI-MS) 2,4-dichlorophenol (2,4-DCP) and 2,4-dichlororesorcinol (2,4-DCR) formation was observed as the main by-products.

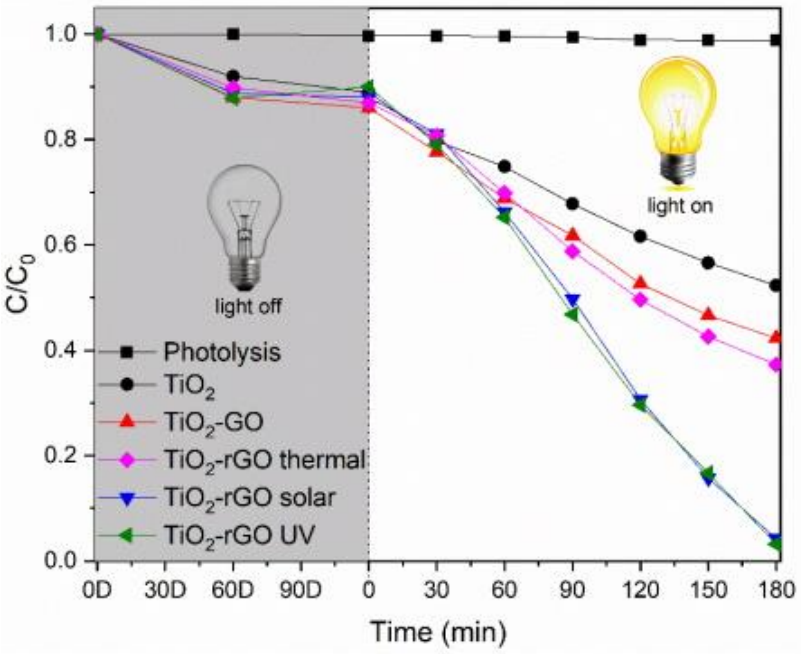


Figure 3. Photodegradation of 2,4-D [84].

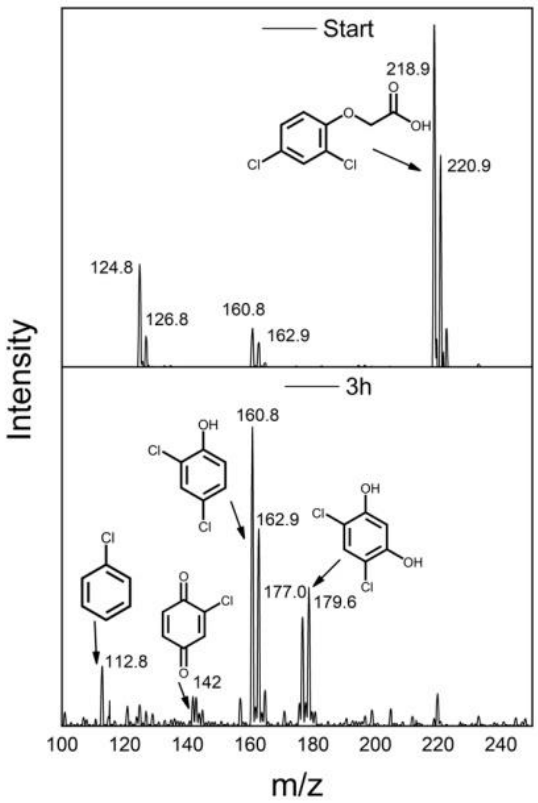


Figure 4. ISI-MS spectra were acquired before the irradiation (**upper spectrum**) and after 3 h of irradiation using the rGO@TiO_2 solar sample (**bottom spectrum**) [84].

In another study, Luna-Sanguino et al. [90] prepared a rGO@TiO_2 nanocomposite that was applied for the removal of methomyl, isoproturon, and alachlor. It was found that rGO@TiO_2 exhibits a high degradation rate after 25 min of natural sunlight irradiation. Deepthi et al. [67] investigated the application of synthesized rGO@TiO_2 nanocomposite for solar-driven degradation of diclofenac (DCF). Besides high effectiveness (>98% DCF degradation and 65% mineralization of organic content within 60 min irradiation), the synthesized rGO@TiO_2 nanocomposite catalyst mineralizes DCF completely in ~100 min. Similar efficiency can be found also for many other degradations [64,68,69,91,92].

Reusability of rGO@TiO_2

The investigation of the long-term stability and reusability of prepared rGO@TiO_2 photocatalyst is a crucial parameter for its practical application. The stability of prepared rGO@TiO_2 photocatalyst is investigated between several consecutive cycles with the same photocatalytic tests. Wanag et al. [25] investigated the stability of prepared rGO@TiO_2 photocatalyst under seven cycles. The obtained results show very high activity after five cycles. A substantial decrease in the photoactivity is noted after seventh cycles. Prepared rGO@TiO_2 photocatalyst showed high stability during the photodegradation of MB dye. In another study, Balsamo et al. [84] investigated the reusability of prepared rGO@TiO_2 solar catalyst under five cycles with very high photodegradation of pesticide. A slight decrease in photoactivity is attributed to the loss of catalyst powder between cycles. Deepthi et al. [67] prepared rGO@TiO_2 catalyst with excellent reusability after six cycles of DCF degradation. Similar reusability of rGO@TiO_2 photocatalyst has been reported in other photodegradation investigations [88,93].

According to published results on photocatalytic degradation of OMPs (dyes, pharmaceuticals, pesticides) and high reusability after several cycles, rGO-based TiO_2 photocatalysts are expected to be commercialized in the near future.

3. Factors Affecting the Photodegradation of Organic Pollutants

Several parameters which affect the photodegradation process are GO to TiO_2 weight ratio, catalyst loading, initial pollutant concentration, pH, water matrix composition, the intensity of irradiation, scavengers, and wavelength of light irradiation. The impact of these parameters is shown in Table 2.

Table 2. The impact of parameters on the rGO@TiO_2 photocatalytic process.

Parameter	Impact on Photocatalysis
Catalyst concentration	The photodegradation rate increases with the increase of the amount of catalyst. Above a certain amount of catalyst, the photodegradation rate decreases as the catalyst amount increases.
Initial pollutant concentration	The photodegradation rate increases with the increase of the initial concentration of pollutant. Above a certain initial concentration of pollutant, the photodegradation rate decreases as the initial concentration of pollutant increases.
pH	The photodegradation rate depends significantly on the pH value.
Light source	Light source supplies irradiation of different wavelengths (UV-C, UV-B, UV-A, visible light, simulated solar light, natural sunlight).

Table 2. *Cont.*

Parameter	Impact on Photocatalysis
Intensity of irradiation	Light intensity depends on the light source and enhances the photocatalytic reaction.
Water matrix	Presence of different pollutants/organic matter that can act as inhibitors or competitors of the photodegradation rate.
Weight ratio of graphene oxide to TiO_2	The photodegradation rate increases with the increasing amount of GO to TiO_2. Above a certain threshold the photodegradation rate decreases as the amount of GO increases.
Scavengers	Improve the separation rate of photogenerated holes and electrons and enhance the photocatalytic reaction.

3.1. The Effect of GO to TiO_2 Weight Ratio

The weight ratio of GO in the rGO@TiO_2 nanocomposite plays a crucial role in obtaining a high surface area. Good TiO_2-decorated rGO sheets can effectively absorb irradiated light and convert it to electron-hole pairs by decreasing the bandgap. The photocatalyst with the most suitable TiO_2 nanoparticles distributed on rGO sheets has the highest charge transfer rate and consequently improves pollutant degradation. Kocijan et al. [63] reported that rGO@TiO_2 nanocomposite with 15 wt.% of GO shows the fastest photodegradation rate of MB and RhB dyes under simulated solar light irradiation. According to Kusiak-Nejman et al. [88], the rGO@TiO_2 with 8 wt.% rGO shows a high rate of MB removal under UV light irradiation.

3.2. Effect of Catalyst Loading

The amount of prepared rGO@TiO_2 photocatalyst can significantly influence the photodegradation rate of the organic pollutant from the aqueous medium. Maruthamani et al. [77] have investigated different concentrations of 20% rGO@TiO_2 in the range of 0.5 to 2.0 g/L to observe the effect of photocatalyst concentration on the degradation rate of RhB (1.25×10^{-4} M) under UV irradiation. The obtained experimental results showed that the catalyst amount has both positive and negative impacts on the photodecomposition rate. The catalysts amount up to 1.5 g/L demonstrated increased photodegradation rate of RhB from 70 to 93%, which could be explained by an increased number of active sites from the catalyst [77]. On the other side, increasing the catalyst amount above, from 1.5 to 2.0 g/L, resulted in a significant drop in photodegradation of RhB. According to their agglomeration of catalyst nanoparticles coupled with increase of suspension turbidity caused light scattering that obstructed UV light penetration during the reaction [83]. Similar results can also be found elsewhere [55,63,84].

3.3. Effect of Initial Pollutant Concentration

Li et al. [93] studied the effect of initial concentration on the degradation of acid orange 7 (AO7) at different concentrations such as 10, 20, and 30 mg/L. The degradation rate decreased with increase of the initial AO7 concentration of up to 30 mg/L. Other papers also reported similar results [68,74]. The effect of initial concentration of RhB dyes on the photodegradation was studied by Maruthamani et al. [77]. They modified the initial concentration of RhB between 0.625×10^{-4} and 5.0×10^{-4} M. They found that the decolourisation percentage of RhB initially increased and later decreased with increase of initial dye concentration. Deepthi et al. [67] investigated the removal rate of diclofenac (DCF) in the initial concentration range of 10–30 mg/L. It was found that the degradation rate of DCF increased steadily for up to 25 mg/L of DCF and thereafter was stabilized or

slightly decreased. Hence, as the organic pollutant concentration increases, more molecules of pollutant are adsorbed on the photocatalyst surface which reduces the surface of active sites, thus fewer photons can reach the catalyst surface. This phenomenon can significantly decrease photocatalytic degradation efficiency due to the reduced production of oxygen reactive species such as $^{\bullet}OH$ and $O_2^{\bullet-}$ radicals [94].

3.4. Effect of Initial pH

The pH value can influence the photodegradation efficiency through several possible reaction mechanisms. Parameters responsible for the changes are substrate and surface chemistry, extent of adsorption, catalyst surface charge, types of surface interactions, substrate nature, solvent molecules, the numerous intermediates formed during the progress of the reaction, etc. [68]. For instance, Deepthi et al. [67] investigated DCF degradation under natural sunlight irradiation, using different initial pH of the DCF solution. A maximum of 68.4% degradation was obtained (using the same rGO@TiO_2 nanocomposite) at pH 6. The point of zero charge (PZC) of the rGO@TiO_2 nanocomposite was found to be at 4.59, meaning that above this pH value the catalyst surface is negatively charged and capable of adsorbing cationic species, whereas below it is positively charged and hence attracts anionic species onto the surface. Thus, the ionic state of the substrate species is vital in determining the adsorption degree and consequently the photodegradation rate. Furthermore, it was observed that pH changes during photocatalytic reactions. According to Balsamo et al. [84], at 3.5 pH (surface with a small positive potential) rGO@TiO_2 nanocomposite showed the highest rate of 2,4-D degradation under solar irradiation. Maruthamani et al. [77] investigated RhB degradation between pH 3.5 and 10.0 and noted that the highest RhB decolorization is under acidic conditions. For pH 3.5 after 3 h under UV light irradiation, the RhB decolorization was at 93%. At pH 10 and above there was also an increase in RhB photodegradation, which was attributed to the fact that the catalyst surface is sufficiently negatively charged. At pH 7 RhB decolorization value was the lowest, which was attributed to the decrease of $TiOH_2^+$ concentration. Deshmukh et al. [65] reported MB degradation using four pH values: 2.3, 4.0, 12.1, and 13.2, as shown in Figure 5. According to the obtained results, as the pH increased from 2.3 to 13.2, the amount of decolorization/degradation of MB dye increased from 17.4 to 91.3% after 30 min of reaction time. The point of zero charge (PZC) of rGO@TiO_2 nanocomposite suspension was measured with the help of zeta potential values at several different pH values and is shown in Figure 5 (inset). The point of zero charge was found to be 2.62 for the ultrasonically prepared rGO@TiO_2 catalyst. At lower pH, the ultrasonically prepared nanocomposite surface got positively charged which led to the protonation of active sites. MB dye is a cationic dye; thus, electrostatic repulsion is generated between the positively charged MB dye molecules and the catalyst surface. Contrarily, at higher pH, the surface of the nanocomposite becomes alkaline in nature which leads to deprotonation. In this case, there is a higher number of negative sites on the surface of the photocatalyst, leading to the interaction of the dye with one of these negative sites on the surface of the nanocomposite.

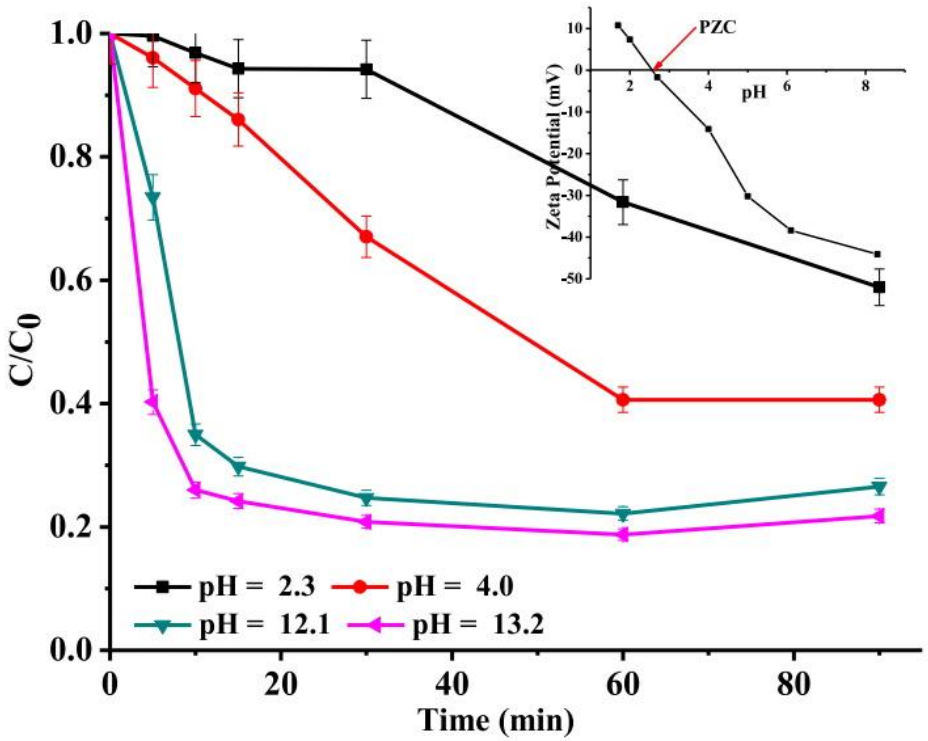


Figure 5. Effect of pH on degradation of MB dye using rGO@TiO_2 nanocomposite. Photocatalyst and zeta potential values at different pH of rGO/TiO_2 suspension (inset). Reprinted with permission from ref. [65]. 2022, Copyright Elsevier.

3.5. Effect of Water Matrix on the Photocatalytic Degradation of Pollutant

Usually, the photocatalytic degradation of organic pollutants throughout the literature was carried out with distilled or ultrapure water, which contains a minimum number of ions, hence also the conductivity was very low. The conductivity of ultrapure and distilled water is between 0.15 and 0.055 μS/cm and 0.5 and 3 μS/cm, respectively [95,96]. The presence of these ions may negatively or positively affect the photodegradation efficiency. For industrial scale-up, the photodegradation efficiency of the system should be tested in various natural water matrices, such as tap water, river water, lake water, seawater, industrial wastewater, etc.

Deepthi et al. [67] investigated the photocatalytic degradation of diclofenac in several water matrices (ultrapure water, river water, dug well water, filtered effluent, and unfiltered effluent) under sunlight irradiation using rGO@TiO_2 nanocomposite. According to their report, they found that DCF can effectively be degraded in all investigated water systems. The photodegradation efficiency decreases in the following order: ultrapure water > river water > dug well water > filtered effluent > unfiltered effluent. Substantial photocatalytic degradation in ultrapure water was finished in 60 min, while it took 90 and 120 min for river and well water, respectively. Four hours were required for the degradation efficiency of only 90% in effluent medium. According to their analysis of the water matrices, the effluent water contained significant amounts of ions (Cl^-, SO_4^{2-}, and PO_4^{3-}). These ions inhibited the photodegradation process. As they argued, ions from effluent water were adsorbed on the catalyst surface, blocking the reactive sites. Furthermore, these ions scavenged holes and hydroxyl radicals producing less powerful oxidants such as NO_3^-, Cl^-, PO_4^{2-}, and CO^{3-}.

3.6. Effect of Intensity and Wavelength of Light Irradiation

TiO_2 has a wide band gap energy (3.0–3.20 eV) which limits its absorption only in the UV region of the solar spectrum. The wavelengths and intensities of UV light irradiation significantly affect the photodegradation of pollutants in an aqueous medium.

UV irradiation is thus more frequently practiced than sunlight as it has higher efficiency in the degradation of pollutants. Expanding the photocatalytic degradation of pollutants to visible irradiation is an important aspect to recon with if we want to commercialize the process. Such a system should be functional under natural sunlight as the irradiation source [97]. The intensity of the light also affects the transition rate of electrons from the valence band (VB) to the conduction band (CB). Higher intensity usually leads to significantly higher degradation rates of the photocatalytic process. After saturation when the amount of photons is equal to TiO_2 active sites, the rate of photogeneration becomes less dependent on the increase of the light intensity. Therefore, appropriate photon energy distribution contributes to the photodegradation rate [9]. A surplus of photons of given energy cannot contribute to a higher photocatalytic degradation rate because of the limited amounts of active sites on the surface of the catalyst [98].

Coupling TiO_2 with materials such as graphene which can shift the response to visible light is crucial for obtaining an effective nanocomposite for photocatalytic applications using natural sunlight irradiation as a cost-effective irradiation source. The synergistic effect between materials in nanocomposites can improve visible light response, charge separation, and photodegradation rate. The reported investigations based on rGO@TiO_2 photocatalyst with different light irradiation are shown in Table 1.

3.7. Effect of Scavengers

The photocatalytic reaction can be enhanced by increasing the number of radicals, which leads to a better separation of charge carriers. These conditions can be created on rGO material which also alters the recombination rate of charge carriers. Furthermore, free oxidative holes can directly react with the organic pollutant compounds or indirectly through the $^{\bullet}OH$ radicals, which are strong oxidants [99]. In an aqueous medium, active components such as hydroxyl radical ($^{\bullet}OH$), holes (h^+), and electrons (e^-) can play significant roles in the photodegradation of organic pollutants.

For instance, Mohammadi et al. [87] investigated photodegradation mechanisms of MB by rGO@TiO_2 under visible light. Several scavengers were introduced. Among them were EDTA for holes (h^+) generation, $AgNO_3$ and $K_2S_2O_8$ for electrons, *p*-benzoquinone for $O_2^{\bullet-}$, *t*-butanol for $^{\bullet}OH$ radical scavenger, and NaN_3 for singlet oxygen, $^1O_2$ species. According to their results, adding *t*-butanol, EDTA and NaN_3 had no considerable influence on the photodegradation of MB dye. They subsequently concluded that OH radicals, h^+, and $^1O_2$ do not play a significant role as active species in MB photodegradation. In contrast, adding e^- through introduction of $K_2S_2O_8$ proved to be the main acetifier of photocatalytic degradation of MB dye. Photocatalytic degradation efficiency decreased in the presence of *p*-benzoquinone, superoxide radical ion, $O_2^{\bullet-}$, which also represents an important finding. Pastrana-Martínez et al. [70] investigated the photodegradation of diphenhydramine under near-UV/Vis and visible light irradiation. EDTA or *t*-BuOH were used as hole and radical trapping agents. It was found that photogenerated holes and hydroxyl radicals are the main reactive species in the investigated process.

The photocatalytic mechanism of the rGO@TiO_2 nanocomposite is shown in Figure 6. rGO in the rGO@TiO_2 nanocomposite can improve photocatalytic degradation of pollutants by promoting separation and charge transfer. The electron-hole pairs have been excited within the TiO_2 molecule after irradiation. The e^- quickly shifted from the CB of the TiO_2 molecule to the surface of the rGO material. Transferred e^- react with dissolved oxygen resulting in the high generation of $^{\bullet}OH$ radicals. Furthermore, the h^+ from the VB of the TiO_2 molecule has the potential to oxidize H_2O/OH^- to form $^{\bullet}OH$ radicals. From the oxidation and reduction process hydroxyl ($^{\bullet}OH$) and superoxide radical ($O_2^{\bullet-}$), are obtained respectively. They react with pollutants (MB dye) to transform pollutants into non-hazardous compounds such as H_2O and CO_2 [66,88,100]. Thus, because of multiple responses of rGO, a careful investigation is crucial to determine under what photocatalytic reaction conditions (such as type of irradiation exposure, pH solution, the concentration of rGO in

the nanocomposite, and nature of oxidizing agent), the photodegradation mechanism of the rGO@TiO_2 nanocomposites can be improved [26,101].

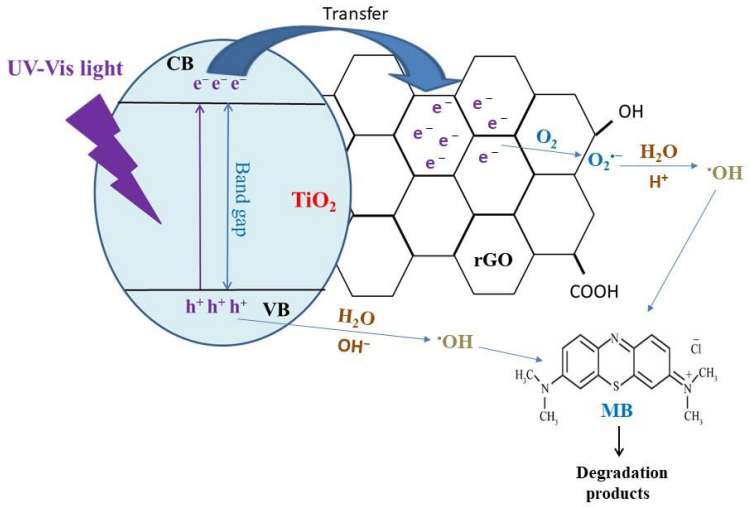


Figure 6. The photocatalytic mechanisms of rGO@TiO_2 nanocomposite for MB dye degradation [99].

4. Challenges and Future Perspectives

With the growth of population and various industries, many pollutants which can have a negative influence on the environment and human health, enter the ecosystem. There is much ongoing research to partially remove pollutants from water and finding an appropriate and effective method is of vital importance. Nowadays, conventional treatments have many drawbacks such as high cost or the formation of toxic by-products. The use of catalysts represents an appealing method to remove pollutants from the water, however, there are still many costs related issues in terms of energy spending.

Advanced oxidation processes especially heterogeneous photocatalytic degradation can be utilized as an appropriate remediation strategy. Heterogeneous catalysts have many advantages over homogeneous catalysts, such as easy separation from the reaction mixture and their reusability. As mentioned above and shown in Table 1, various organic pollutants can be efficiently degraded in natural waters or wastewaters. Among them, rGO@TiO_2 nanocomposite proved to be highly efficient for photodegradation of these contaminants. These novel nanocomposite materials are considered green photocatalysts, and they can be activated by solar light, which avoids pitfalls in consuming energy for the generation of UV light.

In order to realize their full potential, the research gap needs to be closed. First, optimize the integration process of rGO with TiO_2 to further increase the photocatalytic activity using solar irradiation. Fine-tuning the synthesis and photocatalytic parameters is crucial for the large-scale synthesis required for technological implementation. In addition, further research is needed to determine the reversibility of the electronic properties of rGO, as its influence on the photochemical process has not yet been fully elucidated. The use of theoretical models to support empirical models could contribute to obtaining new inputs into the interfacial analysis of the rGO@TiO_2 nanocomposite. Finally, future research should be devoted to investigate the photodegradation of pollutants under realistic conditions and their toxicity in contrast to many published studies under ideal experimental conditions in a short reaction time.

5. Conclusions

This review summarized the progress performed on rGO@TiO_2 catalysts for the photodegradation of organic pollutants from different types of water bodies. Introduced photocatalyst nanocomposite show several advantages. Many studies report different synthesis conditions and there are new strategies for further development. rGO@TiO_2 catalyst

is very versatile in terms of removing different types of contaminants, but also from the applications point of view since it can be prepared as thin films, coatings, etc. Such immobilization of the rGO@TiO_2 catalyst plays an important role for easy recyclability, which is important from the economic aspects. Although many efforts and studies have been made using rGO@TiO_2 as a catalyst there are still some challenges that need to be addressed in the future. Among them and probably the most relevant is the conversion of this technology from a lab to a pilot scale project to finally industrialize this important application.

Author Contributions: Conceptualization, M.K., L.Ć., M.P. and G.G.; writing—original draft preparation, M.K., L.Ć., M.P. and G.G.; writing—review and editing L.Ć., G.G. and M.P. All authors have read and agreed to the published version of the manuscript.

Funding: This research received no external funding.

Institutional Review Board Statement: Not applicable.

Informed Consent Statement: Not applicable.

Data Availability Statement: Not applicable.

Acknowledgments: Gil Gonçalves thank to the Portuguese Science Foundation for the Program Stimulus of Scientific Employment—Individual Support (CEECIND/01913/2017) and the financial support to TEMA (UIDB/00481/2020 and UIDP/00481/2020) and CENTRO-01-0145-FEDER-022083—Centro Portugal Regional Operational Programme (Centro2020), under the PORTUGAL 2020 Partnership Agreement, through the European Regional Development Fund. The financial support of the Slovenian Research Agency is gratefully acknowledged (Project No. L2-1830 and Program No. P2-0084).

Conflicts of Interest: The authors declare no conflict of interest.

Abbreviations

OMPs	organic micropollutants
MB	methylene blue
AOPs	advanced oxidation processes
TiO_2	titanium dioxide
UV	ultraviolet
e^-	electron
h^+	hole
GO	graphene oxide
rGO	reduced graphene oxide
λ	lambda
HNO_3	nitric acid
$KClO_3$	potassium chlorate
H_2SO_4	sulfuric acid
$KMnO_4$	potassium permanganate
$NaNO_3$	sodium nitrate
NO_2	nitrogen dioxide
N_2O_4	dinitrogen tetroxide
ClO_2	chlorine dioxide
TTIP	titanium (IV) isopropoxide
WHO	World Health Organization
MO	methylene orange
Vis	visible
RhB	rhodamine B
Hg	mercury
2,4-D	2,4-dichlorophenoxyacetic acid
ISI-MS	ion-spray ionization mass spectrometry
2,4-DCP	2,4-dichlorophenol
2,4-DCR	dichlororesorcinol

TOC	total organic carbon
DCF	diclofenac
AO7	acid orange 7
$^{\bullet}OH$	hydroxyl radical
$O_2^{\bullet-}$	superoxide radical
PZC	point of zero charge
Cl^-	chloride ion
SO_4^{2-}	sulphate ion
PO_4^{3-}	phosphate ion
NO_3^-	nitrate ion
VB	valence band
CB	conduction band
EDTA	ethylenediaminetetraacetic acid
$AgNO_3$	silver nitrate
$K_2S_2O_8$	potassium persulfate
NaN_3	sodium azide
t-BuOH	tert-butyl alcohol

References

1. Hojjati-Najafabadi, A.; Mansoorianfar, M.; Liang, T.; Shahin, K.; Karimi-Maleh, H. A review on magnetic sensors for monitoring of hazardous pollutants in water resources. *Sci. Total Environ.* **2022**, *824*, 153844. [CrossRef]
2. Karaman, C.; Karaman, O.; Show, P.-L.; Orooji, Y.; Karimi-Maleh, H. Utilization of a double-cross-linked amino-functionalized three-dimensional graphene networks as a monolithic adsorbent for methyl orange removal: Equilibrium, kinetics, thermodynamics and artificial neural network modeling. *Environ. Res.* **2022**, *207*, 112156. [CrossRef] [PubMed]
3. Karaman, C.; Karaman, O.; Show, P.-L.; Karimi-Maleh, H.; Zare, N. Congo red dye removal from aqueous environment by cationic surfactant modified-biomass derived carbon: Equilibrium, kinetic, and thermodynamic modeling, and forecasting via artificial neural network approach. *Chemosphere* **2022**, *290*, 133346. [CrossRef] [PubMed]
4. Orooji, Y.; Tanhaei, B.; Ayati, A.; Tabrizi, S.H.; Alizadeh, M.; Bamoharram, F.F.; Karimi, F.; Salmanpour, S.; Rouhi, J.; Afshar, S.; et al. Heterogeneous UV-Switchable Au nanoparticles decorated tungstophosphoric acid/TiO_2 for efficient photocatalytic degradation process. *Chemosphere* **2021**, *281*, 130795. [CrossRef] [PubMed]
5. Karimi-Maleh, H.; Ayati, A.; Ghanbari, S.; Orooji, Y.; Tanhaei, B.; Karimi, F.; Alizadeh, M.; Rouhi, J.; Fu, L.; Sillanpää, M. Recent advances in removal techniques of Cr(VI) toxic ion from aqueous solution: A comprehensive review. *J. Mol. Liq.* **2021**, *329*, 115062. [CrossRef]
6. Karimi-Maleh, H.; Ranjbari, S.; Tanhaei, B.; Ayati, A.; Orooji, Y.; Alizadeh, M.; Karimi, F.; Salmanpour, S.; Rouhi, J.; Sillanpää, M.; et al. Novel 1-butyl-3-methylimidazomohammadim bromide impregnated chitosan hydrogel beads nanostructure as an efficient nanobio-adsorbent for cationic dye removal: Kinetic study. *Environ. Res.* **2021**, *195*, 110809. [CrossRef]
7. Yaqoob, A.A.; Parveen, T.; Umar, K.; Mohamad Ibrahim, M.N. Role of Nanomaterials in the Treatment of Wastewater: A Review. *Water* **2020**, *12*, 495. [CrossRef]
8. Fernández, C.; Larrechi, M.S.; Callao, M.P. An analytical overview of processes for removing organic dyes from wastewater effluents. *TrAC-Trends Anal. Chem.* **2010**, *29*, 1202–1211. [CrossRef]
9. Chen, D.; Cheng, Y.; Zhou, N.; Chen, P.; Wang, Y.; Li, K.; Huo, S.; Cheng, P.; Peng, P.; Zhang, R.; et al. Photocatalytic degradation of organic pollutants using TiO_2-based photocatalysts: A review. *J. Clean. Prod.* **2020**, *268*, 121725. [CrossRef]
10. Yaqoob, A.A.; Ahmad, H.; Parveen, T.; Ahmad, A.; Oves, M.; Ismail, I.M.I.; Qari, H.A.; Umar, K.; Mohamad Ibrahim, M.N. Recent Advances in Metal Decorated Nanomaterials and Their Various Biological Applications: A Review. *Front. Chem.* **2020**, *8*, 341. [CrossRef]
11. Feng, Z.; Yuan, R.; Wang, F.; Chen, Z.; Zhou, B.; Chen, H. Preparation of magnetic biochar and its application in catalytic degradation of organic pollutants: A review. *Sci. Total Environ.* **2021**, *765*, 142673. [CrossRef]
12. Gusain, R.; Gupta, K.; Joshi, P.; Khatri, O.P. Adsorptive removal and photocatalytic degradation of organic pollutants using metal oxides and their composites: A comprehensive review. *Adv. Colloid Interface Sci.* **2019**, *272*, 102009. [CrossRef]
13. Adeola, A.O.; Abiodun, B.A.; Adenuga, D.O.; Nomngongo, P.N. Adsorptive and photocatalytic remediation of hazardous organic chemical pollutants in aqueous medium: A review. *J. Contam. Hydrol.* **2022**, *248*, 104019. [CrossRef]
14. Maroudas, A.; Pandis, P.K.; Chatzopoulou, A.; Davellas, L.R.; Sourkouni, G.; Argirusis, C. Synergetic decolorization of azo dyes using ultrasounds, photocatalysis and photo-fenton reaction. *Ultrason. Sonochem.* **2021**, *71*, 105367. [CrossRef]
15. Coha, M.; Farinelli, G.; Tiraferri, A.; Minella, M.; Vione, D. Advanced oxidation processes in the removal of organic substances from produced water: Potential, configurations, and research needs. *Chem. Eng. J.* **2021**, *414*, 128668. [CrossRef]
16. Guerra, F.D.; Attia, M.F.; Whitehead, D.C.; Alexis, F. Nanotechnology for environmental remediation: Materials and applications. *Molecules* **2018**, *23*, 1760. [CrossRef]
17. Yaqoob, A.A.; Noor, N.H.; Binti, M.; Umar, K.; Adnan, R.; Ibrahim, M.N.M.; Rashid, M. Graphene oxide–ZnO nanocomposite: An efficient visible light photocatalyst for degradation of rhodamine B. *Appl. Nanosci.* **2021**, *11*, 1291–1302. [CrossRef]

18. Liu, Y.; Su, G.; Zhang, B.; Jiang, G.; Yan, B. Nanoparticle-based strategies for detection and remediation of environmental pollutants. *Analyst* **2011**, *136*, 872–877. [CrossRef]
19. Abdelbasir, S.M.; Shalan, A.E. An overview of nanomaterials for industrial wastewater treatment. *Korean J. Chem. Eng.* **2019**, *36*, 1209–1225. [CrossRef]
20. Yaqoob, A.A.; Habibah, N.; Serr, A.; Nasir, M.; Ibrahim, M. Advances and Challenges in Developing Efficient Graphene Oxide-Based ZnO Photocatalysts for Dye Photo-Oxidation. *Nanomaterials* **2020**, *10*, 932. [CrossRef]
21. Du, X.; Luo, J.; Qin, Q.; Zhang, J.; Fu, D. Modified TiO_2-rGO Binary Photo-Degradation Nanomaterials: Modification, Mechanism, and Perspective. *Catal. Surv. Asia* **2022**, *26*, 16–34. [CrossRef]
22. Schneider, J.; Matsuoka, M.; Takeuchi, M.; Zhang, J.; Horiuchi, Y.; Anpo, M.; Bahnemann, D.W. Understanding TiO_2 Photocatalysis: Mechanisms and Materials. *Chem. Rev.* **2014**, *114*, 9919–9986. [CrossRef] [PubMed]
23. Pelaez, M.; Nolan, N.T.; Pillai, S.C.; Seery, M.K.; Falaras, P.; Kontos, A.G.; Dunlop, P.S.M.; Hamilton, J.W.J.; Byrne, J.A.; O'Shea, K.; et al. A review on the visible light active titanium dioxide photocatalysts for environmental applications. *Appl. Catal. B Environ.* **2012**, *125*, 331–349. [CrossRef]
24. Ren, G.; Han, H.; Wang, Y.; Liu, S.; Zhao, J.; Meng, X.; Li, Z. Recent Advances of Photocatalytic Application in Water Treatment: A Review. *Nanomaterials* **2021**, *11*, 1804. [CrossRef] [PubMed]
25. Wanag, A.; Kusiak-Nejman, E.; Czyżewski, A.; Moszyński, D.; Morawski, A.W. Influence of rGO and preparation method on the physicochemical and photocatalytic properties of TiO_2/reduced graphene oxide photocatalysts. *Catalysts* **2021**, *11*, 1333. [CrossRef]
26. Padmanabhan, N.T.; Thomas, N.; Louis, J.; Mathew, D.T.; Ganguly, P.; John, H.; Pillai, S.C. Graphene coupled TiO_2 photocatalysts for environmental applications: A review. *Chemosphere* **2021**, *271*, 129506. [CrossRef]
27. Tong, H.; Ouyang, S.; Bi, Y.; Umezawa, N.; Oshikiri, M.; Ye, J. Nano-photocatalytic Materials: Possibilities and Challenges. *Adv. Mater.* **2012**, *24*, 229–251. [CrossRef]
28. Tatarchuk, T.; Peter, A.; Al-Najar, B.; Vijaya, J.; Bououdina, M. Photocatalysis: Activity of Nanomaterials. In *Nanotechnology in Environmental Science*; Wiley: Hoboken, NJ, USA, 2018; pp. 209–292.
29. Xie, X.; Kretschmer, K.; Wang, G. Advances in graphene-based semiconductor photocatalysts for solar energy conversion: Fundamentals and materials engineering. *Nanoscale* **2015**, *7*, 13278–13292. [CrossRef]
30. Xiang, Q.; Yu, J.; Jaroniec, M. Graphene-based semiconductor photocatalysts. *Chem. Soc. Rev.* **2012**, *41*, 782–796. [CrossRef]
31. Allen, J.M.; Vincent, T.C.; Richard, K.B. Honeycomb carbon: A Review of Graphene What is graphene? *Chem. Rev.* **2010**, *110*, 132–145. [CrossRef]
32. Pastrana-Martínez, L.M.; Morales-Torres, S.; Figueiredo, J.L.; Faria, J.L.; Silva, A.M.T. Graphene Derivatives in Photocatalysis. In *Graphene-Based Energy Devices*; Wiley: Hoboken, NJ, USA, 2015; pp. 249–276. [CrossRef]
33. Razaq, A.; Bibi, F.; Zheng, X.; Papadakis, R.; Jafri, S.H.M.; Li, H. Review on Graphene-, Graphene Oxide-, Reduced Graphene Oxide-Based Flexible Composites: From Fabrication to Applications. *Materials* **2022**, *15*, 1012. [CrossRef]
34. Dideikin, A.T.; Vul, A.Y. Graphene oxide and derivatives: The place in graphene family. *Front. Phys.* **2019**, *6*. [CrossRef]
35. Bianco, A.; Cheng, H.M.; Enoki, T.; Gogotsi, Y.; Hurt, R.H.; Koratkar, N.; Kyotani, T.; Monthioux, M.; Park, C.R.; Tascon, J.M.D.; et al. All in the graphene family-A recommended nomenclature for two-dimensional carbon materials. *Carbon* **2013**, *65*, 1–6. [CrossRef]
36. Eigler, S. Mechanistic insights into the reduction of graphene oxide addressing its surfaces. *Phys. Chem. Chem. Phys.* **2014**, *16*, 19832–19835. [CrossRef]
37. Li, F.; Jiang, X.; Zhao, J.; Zhang, S. Graphene oxide: A promising nanomaterial for energy and environmental applications. *Nano Energy* **2015**, *16*, 488–515. [CrossRef]
38. Guex, L.G.; Sacchi, B.; Peuvot, K.F.; Andersson, R.L.; Pourrahimi, A.M.; Ström, V.; Farris, S.; Olsson, R.T. Experimental review: Chemical reduction of graphene oxide (GO) to reduced graphene oxide (rGO) by aqueous chemistry. *Nanoscale* **2017**, *9*, 9562–9571. [CrossRef] [PubMed]
39. Agarwal, V.; Zetterlund, P.B. Strategies for reduction of graphene oxide–A comprehensive review. *Chem. Eng. J.* **2021**, *405*, 127018. [CrossRef]
40. Oliveira, A.M.L.; Machado, M.; Silva, G.A.; Bitoque, D.B.; Ferreira, J.T.; Ferreira, Q. Graphene Oxide Thin Films with Drug Delivery Function. *Nanomaterials* **2022**, *12*, 1149. [CrossRef] [PubMed]
41. Brodie, B.C. On the Atomic Weight of Graphite. *Philos. Trans. R. Soc. Lond.* **1859**, *149*, 249–259.
42. Staudenmaier, L. Method for the preparation of the graphite acid. *Eur. J. Inorg. Chem.* **1898**, *31*, 1481–1487.
43. Hummers, W.S.; Offeman, R.E. Preparation of Graphitic Oxide. *J. Am. Chem. Soc.* **1958**, *80*, 1339. [CrossRef]
44. Al Kausor, M.; Chakrabortty, D. Graphene oxide based semiconductor photocatalysts for degradation of organic dye in waste water: A review on fabrication, performance enhancement and challenges. *Inorg. Chem. Commun.* **2021**, *129*, 108630. [CrossRef]
45. Marcano, D.C.; Kosynkin, D.V.; Berlin, J.M.; Sinitskii, A.; Sun, Z.; Slesarev, A.; Alemany, L.B.; Lu, W.; Tour, J.M. Improved synthesis of graphene oxide. *ACS Nano* **2010**, *4*, 4806–4814. [CrossRef]
46. Sabzevari, M.; Cree, D.; Wilson, L. Preparation and Characterization of Graphene Oxide Cross-Linked Composites. In Proceedings of the CSME Conference Proceedings, Toronto, ON, Canada, 27–30 May 2018. [CrossRef]
47. Zaaba, N.I.; Foo, K.L.; Hashim, U.; Tan, S.J.; Liu, W.W.; Voon, C.H. Synthesis of Graphene Oxide using Modified Hummers Method: Solvent Influence. *Procedia Eng.* **2017**, *184*, 469–477. [CrossRef]

48. Alam, S.N.; Sharma, N.; Kumar, L. Synthesis of Graphene Oxide (GO) by Modified Hummers Method and Its Thermal Reduction to Obtain Reduced Graphene Oxide (rGO). *Graphene* **2017**, *6*, 1–18. [CrossRef]
49. Yu, H.; Zhang, B.; Bulin, C.; Li, R.; Xing, R. High-efficient Synthesis of Graphene Oxide Based on Improved Hummers Method. *Sci. Rep.* **2016**, *6*, 36143. [CrossRef] [PubMed]
50. Paulchamy, B.; Arthi, G.; Lignesh, B.D. A Simple Approach to Stepwise Synthesis of Graphene Oxide Nanomaterial. *J. Nanomed. Nanotechnol.* **2015**, *6*, 1–4. [CrossRef]
51. Gao, X.; Jang, J.; Nagase, S. Hydrazine and thermal reduction of graphene oxide: Reaction mechanisms, product structures, and reaction design. *J. Phys. Chem. C* **2010**, *114*, 832–842. [CrossRef]
52. Chua, C.K.; Pumera, M. Chemical reduction of graphene oxide: A synthetic chemistry viewpoint. *Chem. Soc. Rev.* **2014**, *43*, 291–312. [CrossRef]
53. Sengupta, I.; Chakraborty, S.; Talukdar, M.; Pal, S.K.; Chakraborty, S. Thermal reduction of graphene oxide: How temperature influences purity. *J. Mater. Res.* **2018**, *33*, 4113–4122. [CrossRef]
54. Anandan, S.; Manivel, A.; Ashokkumar, M. One-step sonochemical synthesis of reduced graphene oxide/Pt/Sn hybrid materials and their electrochemical properties. *Fuel Cells* **2012**, *12*, 956–962. [CrossRef]
55. Viinikanoja, A.; Wang, Z.; Kauppila, J.; Kvarnström, C. Electrochemical reduction of graphene oxide and its in situ spectroelectrochemical characterization. *Phys. Chem. Chem. Phys.* **2012**, *14*, 14003–14009. [CrossRef]
56. Quezada Renteria, J.A.; Ruiz-Garcia, C.; Sauvage, T.; Chazaro-Ruiz, L.F.; Rangel-Mendez, J.R.; Ania, C.O. Photochemical and electrochemical reduction of graphene oxide thin films: Tuning the nature of surface defects. *Phys. Chem. Chem. Phys.* **2020**, *22*,20732–20743. [CrossRef] [PubMed]
57. McAllister, M.J.; Li, J.-L.; Adamson, D.H.; Schniepp, H.C.; Abdala, A.A.; Liu, J.; Herrera-Alonso, M.; Milius, D.L.; Car, R.; Prud'homme, R.K.; et al. Single Sheet Functionalized Graphene by Oxidation and Thermal Expansion of Graphite. *Chem. Mater.* **2007**, *19*, 4396–4404. [CrossRef]
58. Stepić, K.; Ljupković, R.; Ickovski, J.; Zarubica, A. A short review of titania-graphene oxide-based composites as a photocatalysts. *Adv. Technol.* **2021**, *10*, 51–60. [CrossRef]
59. Das, A.; Adak, M.K.; Mahata, N.; Biswas, B. Wastewater treatment with the advent of TiO_2 endowed photocatalysts and their reaction kinetics with scavenger effect. *J. Mol. Liq.* **2021**, *338*, 116479. [CrossRef]
60. Hu, Y.; Zhou, C.; Wang, H.; Chen, M.; Zeng, G.; Liu, Z.; Liu, Y.; Wang, W.; Wu, T.; Shao, B.; et al. Recent advance of graphene/semiconductor composite nanocatalysts: Synthesis, mechanism, applications and perspectives. *Chem. Eng. J.* **2021**, *414*, 128795. [CrossRef]
61. Preetha, S.; Pillai, R.; Ramamoorthy, S.; Mayeen, A.; Archana, K.M.; Kalarikkal, N.; Narasimhamurthy, B.; Lekshmi, I.C. TiO_2–rGO Nanocomposites with high rGO content and Luminescence Quenching through Green Redox Synthesis. *Surf. Interfaces* **2022**, *30*, 101812. [CrossRef]
62. Dutta, V.; Singh, P.; Shandilya, P.; Sharma, S.; Raizada, P.; Saini, A.K.; Gupta, V.K.; Hosseini-Bandegharaei, A.; Agarwal, S.; Rahmani-Sani, A. Review on advances in photocatalytic water disinfection utilizing graphene and graphene derivatives-based nanocomposites. *J. Environ. Chem. Eng.* **2019**, *7*, 103132. [CrossRef]
63. Kocijan, M.; Ćurković, L.; Ljubas, D.; Mužina, K.; Bačić, I.; Radošević, T.; Podlogar, M.; Bdikin, I.; Otero-Irurueta, G.; Hortigüela, M.J.; et al. Graphene-Based TiO2 Nanocomposite for Photocatalytic Degradation of Dyes in Aqueous Solution under Solar-Like Radiation. *Appl. Sci.* **2021**, *11*, 3966. [CrossRef]
64. Sohail, M.; Xue, H.; Jiao, Q.; Li, H.; Khan, K.; Wang, S.; Zhao, Y. Synthesis of well-dispersed TiO_2@reduced graphene oxide (rGO) nanocomposites and their photocatalytic properties. *Mater. Res. Bull.* **2017**, *90*, 125–130. [CrossRef]
65. Deshmukh, S.P.; Kale, D.P.; Kar, S.; Shirsath, S.R.; Bhanvase, B.A.; Saharan, V.K.; Sonawane, S.H. Ultrasound assisted preparation of rGO/TiO_2 nanocomposite for effective photocatalytic degradation of methylene blue under sunlight. *Nano-Struct. Nano-Objects* **2020**, *21*, 100407. [CrossRef]
66. Garrafa-Gálvez, H.E.; Alvarado-Beltrán, C.G.; Almaral-Sánchez, J.L.; Hurtado-Macías, A.; Garzon-Fontecha, A.M.; Luque, P.A.; Castro-Beltrán, A. Graphene role in improved solar photocatalytic performance of TiO_2-RGO nanocomposite. *Chem. Phys.* **2019**, *521*, 35–43. [CrossRef]
67. Deepthi, J.; Rajalakshmi, A.S.; Lopez, R.M.; Achari, V.S. TiO_2-reduced graphene oxide nanocomposites for the trace removal of diclofenac. *SN Appl. Sci.* **2020**, *2*, 480. [CrossRef]
68. Xu, L.; Yang, L.; Johansson, E.M.J.; Wang, Y.; Jin, P. Photocatalytic activity and mechanism of bisphenol a removal over TiO_2-x/rGO nanocomposite driven by visible light. *Chem. Eng. J.* **2018**, *350*, 1043–1055. [CrossRef]
69. Zhou, Q.; Zhong, Y.H.; Chen, X.; Huang, X.J.; Wu, Y.C. Mesoporous anatase TiO_2/reduced graphene oxide nanocomposites: A simple template-free synthesis and their high photocatalytic performance. *Mater. Res. Bull.* **2014**, *51*, 244–250. [CrossRef]
70. Pastrana-Martínez, L.M.; Morales-Torres, S.; Likodimos, V.; Figueiredo, J.L.; Faria, J.L.; Falaras, P.; Silva, A.M.T. Advanced nanostructured photocatalysts based on reduced graphene oxide-TiO_2 composites for degradation of diphenhydramine pharmaceutical and methyl orange dye. *Appl. Catal. B Environ.* **2012**, *123–124*, 241–256. [CrossRef]
71. Tolosana-Moranchel, Á.; Manassero, A.; Satuf, M.L.; Alfano, O.M.; Casas, J.A.; Bahamonde, A. Influence of TiO_2-rGO optical properties on the photocatalytic activity and efficiency to photodegrade an emerging pollutant. *Appl. Catal. B Environ.* **2019**, *246*, 1–11. [CrossRef]

72. Leal, J.F.; Cruz, S.M.A.; Almeida, B.T.A.; Esteves, V.I.; Marques, P.A.A.P.; Santos, E.B.H. TiO_2-rGO nanocomposite as an efficient catalyst to photodegrade formalin in aquaculture's waters, under solar light. *Environ. Sci. Water Res. Technol.* **2020**, *6*, 1018–1027. [CrossRef]
73. Sun, X.; Ji, S.; Wang, M.; Dou, J.; Yang, Z.; Qiu, H.; Kou, S.; Ji, Y.; Wang, H. Fabrication of porous TiO_2-rGO hybrid aerogel for high-efficiency, visible-light photodegradation of dyes. *J. Alloys Compd.* **2020**, *819*, 153033. [CrossRef]
74. H.H. Ali, M.; E Goher, M.; D.G. Al-Afify, A. Kinetics and Adsorption Isotherm Studies of Methylene Blue Photodegradation Under UV Irradiation Using Reduced Graphene Oxide-TiO_2 Nanocomposite in Different Wastewaters Effluents. *Egypt. J. Aquat. Biol. Fish.* **2019**, *23*, 253–263. [CrossRef]
75. Zhang, Y.; Fu, F.; Zhou, F.; Yang, X.; Zhang, D.; Chen, Y. Synergistic effect of rGO/TiO_2 nanosheets with exposed (001) facets for boosting visible light photocatalytic activity. *Appl. Surf. Sci.* **2020**, *510*, 145451. [CrossRef]
76. Duan, Y.; Gou, M.L.; Guo, Y.; Cai, J.; Song, W.; Liu, Z.; Zhou, E. In situ hydrothermal synthesis of TiO_2–rGO nanocomposites for 4-nitrophenol degradation under sunlight irradiation. *J. Mater. Res.* **2021**, *36*, 906–915. [CrossRef]
77. Maruthamani, D.; Divakar, D.; Kumaravel, M. Enhanced photocatalytic activity of TiO_2 by reduced graphene oxide in mineralization of Rhodamine B dye. *J. Ind. Eng. Chem.* **2015**, *30*, 33–43. [CrossRef]
78. Abd Elnaby, M.; Ahmed, M.A.; Abdel-Samad, H.S.; Hesham Medien, M. Exceptional removal of methylene blue dye over novel TiO_2/rGO nanocomposites by tandem adsorption-photocatalytic processes. *Mater. Sci. Energy Technol.* **2022**, *5*, 217–231. [CrossRef]
79. Fan, H.; Yi, G.; Zhang, Z.; Zhang, X.; Li, P.; Zhang, C.; Chen, L.; Zhang, Y.; Sun, Q. Binary TiO_2/rGO photocatalyst for enhanced degradation of phenol and its application in underground coal gasification wastewater treatment. *Opt. Mater.* **2021**, *120*, 111482. [CrossRef]
80. Zhou, X.; Zhou, S.; Ma, F.; Xu, Y. Synergistic effects and kinetics of rGO-modified TiO_2 nanocomposite on adsorption and photocatalytic degradation of humic acid. *J. Environ. Manag.* **2019**, *235*, 293–302. [CrossRef]
81. Sun, N.; Ma, J.; Wang, C.; Xue, J.; Qiang, L.; Tang, J. A facile and efficient method to directly synthesize TiO_2/rGO with enhanced photocatalytic performance. *Superlattices Microstruct.* **2018**, *121*, 1–8. [CrossRef]
82. Ruidíaz-Martínez, M.; Álvarez, M.A.; López-Ramón, M.V.; Cruz-Quesada, G.; Rivera-Utrilla, J.; Sánchez-Polo, M. Hydrothermal Synthesis of rGO-TiO_2 Composites as High-Performance UV Photocatalysts for Ethylparaben Degradation. *Catalysts* **2020**, *10*, 520. [CrossRef]
83. Yu, F.; Bai, X.; Yang, C.; Xu, L.; Ma, J. Reduced Graphene Oxide–P25 Nanocomposites as Efficient Photocatalysts for Degradation of Bisphenol A in Water. *Catalysts* **2019**, *9*, 607. [CrossRef]
84. Balsamo, S.A.; Fiorenza, R.; Condorelli, M.; Pecoraro, R.; Brundo, M.V.; Presti, F.L.; Scir, S. One-Pot Synthesis of TiO_2-rGO Photocatalysts for the Degradation of Groundwater Pollutants. *Materials* **2021**, *14*, 5938. [CrossRef]
85. Sohail, M.; Saleem, M.; Ullah, S.; Saeed, N.; Afridi, A.; Khan, M.; Arif, M. Modified and improved Hummer's synthesis of graphene oxide for capacitors applications. *Mod. Electron. Mater.* **2017**, *3*, 110–116. [CrossRef]
86. Liu, Y. Hydrothermal synthesis of TiO_2-RGO composites and their improved photocatalytic activity in visible light. *RSC Adv.* **2014**, *4*, 36040–36045. [CrossRef]
87. Mohammadi, M.; Rezaee Roknabadi, M.; Behdani, M.; Kompany, A. Enhancement of visible and UV light photocatalytic activity of rGO-TiO_2 nanocomposites: The effect of TiO_2/Graphene oxide weight ratio. *Ceram. Int.* **2019**, *45*, 12625–12634. [CrossRef]
88. Kusiak-Nejman, E.; Wanag, A.; Kapica- Kozar, J.; Kowalczyk, Ł.; Zgrzebnicki, M.; Tryba, B.; Przepiórski, J.; Morawski, A.W. Methylene blue decomposition on TiO_2/reduced graphene oxide hybrid photocatalysts obtained by a two-step hydrothermal and calcination synthesis. *Catal. Today* **2019**, *357*, 630–637. [CrossRef]
89. Wu, S.; Jia, Q.; Dai, W. Synthesis of rGO/TiO_2 hybrid as a high performance photocatalyst. *Ceram. Int.* **2017**, *43*, 1530–1535. [CrossRef]
90. Luna-Sanguino, G.; Ruíz-Delgado, A.; Tolosana-Moranchel, A.; Pascual, L.; Malato, S.; Bahamonde, A.; Faraldos, M. Solar photocatalytic degradation of pesticides over TiO_2-rGO nanocomposites at pilot plant scale. *Sci. Total Environ.* **2020**, *737*, 140286. [CrossRef]
91. Ton, N.N.T.; Dao, A.T.N.; Kato, K.; Ikenaga, T.; Trinh, D.X.; Taniike, T. One-pot synthesis of TiO_2/graphene nanocomposites for excellent visible light photocatalysis based on chemical exfoliation method. *Carbon* **2018**, *133*, 109–117. [CrossRef]
92. Liang, D.; Cui, C.; Hub, H.; Wang, Y.; Xu, S.; Ying, B.; Li, P.; Lu, B.; Shen, H. One-step hydrothermal synthesis of anatase TiO_2/reduced graphene oxide nanocomposites with enhanced photocatalytic activity. *J. Alloys Compd.* **2014**, *582*, 236–240. [CrossRef]
93. Li, T.; Wang, T.; Qu, G.; Liang, D.; Hu, S. Synthesis and photocatalytic performance of reduced graphene oxide–TiO_2 nanocomposites for orange II degradation under UV light irradiation. *Environ. Sci. Pollut. Res.* **2017**, *24*, 12416–12425. [CrossRef]
94. Zhao, D.; Sheng, G.; Chen, C.; Wang, X. Enhanced photocatalytic degradation of methylene blue under visible irradiation on graphene@TiO_2 dyade structure. *Appl. Catal. B Environ.* **2012**, *111–112*, 303–308. [CrossRef]
95. Zhang, X.; Yang, Y.; Ngo, H.H.; Guo, W.; Wen, H.; Wang, X.; Zhang, J.; Long, T. A critical review on challenges and trend of ultrapure water production process. *Sci. Total Environ.* **2021**, *785*, 147254. [CrossRef] [PubMed]
96. Díez, A.M.; Pazos, M.; Sanromán, M.A. Synthesis of magnetic-photo-Fenton catalyst for degradation of emerging pollutant. *Catal. Today* **2019**, *328*, 267–273. [CrossRef]

97. Reza, K.M.; Kurny, A.; Gulshan, F. Parameters affecting the photocatalytic degradation of dyes using TiO_2: A review. *Appl. Water Sci.* **2017**, *7*, 1569–1578. [CrossRef]
98. Cheng, H.Y.; Chang, K.C.; Lin, K.L.; Ma, C.M. Study on isopropanol degradation by UV/TiO_2 nanotube. *AIP Conf. Proc.* **2018**, *1946*, 020006. [CrossRef]
99. Kocijan, M.; Ćurković, L.; Bdikin, I.; Otero-Irurueta, G.; Hortigüela, M.J.; Gonçalves, G.; Radošević, T.; Vengust, D.; Podlogar, M. Immobilised rGO/TiO_2 Nanocomposite for Multi-Cycle Removal of Methylene Blue Dye from an Aqueous Medium. *Appl. Sci.* **2022**, *12*, 385. [CrossRef]
100. Muthirulan, P.; Devi, C.N.; Sundaram, M.M. TiO_2 wrapped graphene as a high performance photocatalyst for acid orange 7 dye degradation under solar/UV light irradiations. *Ceram. Int.* **2014**, *40*, 5945–5957. [CrossRef]
101. Mondal, A.; Prabhakaran, A.; Gupta, S.; Subramanian, V.R. Boosting Photocatalytic Activity Using Reduced Graphene Oxide (rGO)/Semiconductor Nanocomposites: Issues and Future Scope. *ACS Omega* **2021**, *6*, 8734–8743. [CrossRef]